Photosynth Res (2013) 117:375–383
DOI 10.1007/s11120-013-9939-6

REGULAR PAPER

Crystal structure of the Psb28 accessory factor of *Thermosynechococcus elongatus* photosystem II at 2.3 Å

Wojciech Bialek · Songjia Wen · Franck Michoux · Martina Beckova · Josef Komenda · James W. Murray · Peter J. Nixon

Received: 6 June 2013 / Accepted: 2 October 2013 / Published online: 15 October 2013

Abstract Members of the Psb28 family of proteins are accessory factors implicated in the assembly and repair of the photosystem II complex. We present here the crystal structure of the Psb28 protein (Tlr0493) found in the thermophilic cyanobacterium *Thermosynechococcus elongatus* at a resolution of 2.3 Å. Overall the crystal structure of the Psb28 monomer is similar to the solution structures of C-terminally His-tagged Psb28-1 from *Synechocystis* sp. PCC 6803 obtained previously by nuclear magnetic resonance spectroscopy. One new aspect is that *Escherichia coli*-expressed *T. elongatus* Psb28 is able to form dimers in solution and packs as a dimer of dimers in the crystal. Analysis of wild type and mutant strains of *Synechocystis* 6803 by blue native-polyacrylamide gel electrophoresis suggests that Psb28-1, the closest homologue to *T. elongatus* Psb28 in this organism, also exists as an oligomer in vivo, most likely a dimer. In line with the prediction based on the crystal structure of *T. elongatus* Psb28, the addition of a 3× Flag-tag to the C-terminus of *Synechocystis* 6803 Psb28-1 interferes with the accumulation of the Psb28-1 oligomer in vivo. In contrast, the more distantly related Psb28-2 protein found in *Synechocystis* 6803 lacks the residues that stabilize dimer formation in the *T. elongatus* Psb28 crystal and is detected as a monomer in vivo. Overall our data suggest that the dimer interface in the Psb28 crystal might be physiologically relevant.

Keywords Assembly factor · Psb28 · Psb28-2 · X-ray crystallography · Photosystem II · Cyanobacteria

Abbreviations

D1	Photosystem II reaction center subunit encoded by *psbA*
D2	Photosystem II reaction center subunit encoded by *psbD*
CP43 and CP47	Photosystem II proximal light-harvesting subunits encoded by *psbC* and *psbB*, respectively
RC47	Photosystem II complex lacking CP43
RCC1	Monomeric photosystem II
RCC2	Dimeric photosystem II
RMSD	Root mean square deviation

Introduction

The Photosystem II (PSII) complex, which functions as the light-driven water: plastoquinone oxidoreductase of oxygenic

Electronic supplementary material The online version of this article (doi:10.1007/s11120-013-9939-6) contains supplementary material, which is available to authorized users.

W. Bialek · S. Wen · F. Michoux · J. W. Murray · P. J. Nixon (✉)
Sir Ernst Chain Building–Wolfson Laboratories, Department of Life Sciences, Imperial College London, South Kensington Campus, London SW7 2AZ, UK
e-mail: p.nixon@imperial.ac.uk

Present Address:
S. Wen
Department of Biochemistry, LKS Faculty of Medicine, The University of Hong Kong, Pokfulam, Hong Kong, China

Present Address:
F. Michoux
Alkion Biopharma, 4 Rue Pierre Fontaine, 91058 Evry, France

M. Beckova
Faculty of Science, University of South Bohemia, Branisovska 31, Ceske Budejovice, Czech Republic

J. Komenda
Institute of Microbiology, Academy of Sciences, 379 81 Trebon, Czech Republic

photosynthesis, is found in the thylakoid membrane system of cyanobacteria and chloroplasts. Crystal structures of isolated dimeric oxygen-evolving PSII complexes have been determined for the cyanobacteria *Thermosynechococcus elongatus* and *Thermosynechococcus vulcanus* (Kamiya and Shen 2003; Ferreira et al. 2004; Loll et al. 2005; Guskov et al. 2009; Umena et al. 2011). In the case of *T. elongatus*, each monomer is composed of 17 intrinsic and 3 extrinsic subunits and a variety of cofactors (Guskov et al. 2009). Recent studies have begun to reveal how PSII is assembled from its component parts. Current evidence suggests a modular assembly of PSII (Nixon et al. 2010; Boehm et al. 2011). First, a PSII reaction centre (PSII RC) complex is formed from PsbI-precursor D1 (Dobakova et al. 2007) and cytochrome b_{559}-D2 (Komenda et al. 2004) sub-complexes. Then a CP47 module (Boehm et al. 2011) is attached to create the RC47 complex, after which a CP43 module (Boehm et al. 2011) is added to form the non-oxygen-evolving monomeric PSII complex. At this stage, the oxygen-evolving Mn_4CaO_5 cluster is assembled; the PsbO, PsbU and PsbV lumenal extrinsic proteins are attached and PSII can dimerise (reviewed by Komenda et al. 2012a). Removal of the C-terminal extension of the precursor D1 subunit (Komenda et al. 2007), which is required for assembly of the Mn_4CaO_5 cluster (Nixon et al. 1992), is initiated in vivo after formation of the PSII RC (Komenda et al. 2004).

The PSII complex is susceptible to light-induced damage, which can lead to chronic photoinhibition (Adir et al. 2003). Damaged subunits, predominantly the D1 subunit, are replaced during the so-called 'PSII repair cycle'. Current models suggest that the damaged PSII complex partially disassembles to form the monomeric RC47 complex (Komenda et al. 2004); the damaged D1 protein is degraded by a hetero-oligomeric FtsH protease complex (Boehm et al. 2012a) and replaced by a newly synthesised copy of D1. Oxygen-evolving monomeric and dimeric complexes are then reformed as in PSII assembly (Komenda et al. 2012a).

A number of accessory factors have been identified in various types of PSII complex that are absent in the crystallised dimeric PSII complex (Nixon et al. 2010; Chi et al. 2012). Their functions are still unclear, but current evidence suggests roles in the assembly and repair of PSII or the optimisation of water oxidation. One of these, Psb28-1, encoded by sll1398 in *Synechocystis* sp. PCC 6803 (hereafter *Synechocystis* 6803), is known to bind to the cytoplasmic surface of PSII close to CP47 and PsbH (Dobakova et al. 2009) and in the vicinity of the HliB and HliC subunits that can attach to PSII in vivo (Promnares et al. 2006; Yao et al. 2007). Psb28-1 is mainly found in RC47 complexes in WT (Dobakova et al. 2009) and has been recently detected in isolated PSII core complexes containing the His-tagged Psb27 subunit (Liu et al. 2011). Analysis of a *psb28-1* null mutant of *Synechocystis* 6803 has led to the hypothesis that Psb28-1 might be involved in the synthesis of chlorophylls and/or the apopolypeptides of the chlorophyll-binding proteins CP47 and PsaA/PsaB (Dobakova et al. 2009) although this phenotype appears to be dependent on the particular WT strain used (Sakata et al. 2013). In addition, Psb28-1 is involved in maintaining PSII activity during heat stress possibly at the level of repair (Sakata et al. 2013). *Synechocystis* 6803, like certain other cyanobacteria, also encodes a second Psb28 homologue, designated Psb28-2, encoded by slr1739, which has also been detected in RC47 complexes (Boehm et al. 2012b).

The structure of a C-terminally His-tagged derivative of Psb28-1 encoded by *Synechocystis* 6803 has been determined by nuclear magnetic resonance spectroscopy (NMR) (Yang et al. 2011). Here, we present the crystal structure of the single Psb28 homologue found in the thermophilic cyanobacterium *T. elongatus* which has also been reported to associate with PSII (Nowaczyk et al. 2012). As anticipated, the overall fold of Psb28 is conserved between the two species. However, our results suggest that Psb28-1 might actually exist as a dimer in vivo and that dimerization is impaired by addition of protein tags at the C-terminus.

Materials and methods

Cloning, expression and purification of Psb28

A PCR fragment containing the Psb28 gene of *T. elongatus* (*tlr0493*) was amplified from genomic DNA using Phusion polymerase (NEB, UK) and primers Psb28-BamHI-F (5′-TATATAGGATCCGGTGCAATGGCAGAAATT-3′) and Psb28-EcoRI-R (5′-TATATA GAATTCTTATCAAGAGT TCTCAGACTTCTGAAAGCCA-3′), purified, digested by BamHI/EcoRI and ligated (Quick Ligation Kit, New England Biolabs, UK) into a modified version of pRSET-A that directs the expression of a target protein with a thrombin-cleavable N-terminal His_6-tag (Michoux et al. 2010). Soluble His_6-tagged Psb28 was expressed in the KRX strain of *Escherichia coli*, purified using immobilised Ni^{2+}-affinity chromatography and the His-tag removed by thrombin cleavage as described by Michoux et al. (2012). Size-exclusion chromatography was performed on a Superdex75 10/300 GL column (GE Healthcare) equilibrated with 50 mM Tris pH 8.0, 150 mM NaCl or 50 mM MES pH 6.5, 5 mM $MgCl_2$, 5 mM $CaCl_2$. The column was calibrated for each buffer with molecular weight markers for gel filtration chromatography from Sigma (BSA, carbonic anhydrase, cytochrome *c* and aprotinin).

Crystallization and structure solution

The protein lacking the hexahistidine tag was concentrated to 32 mg/ml and crystallisation screens were set up at 19 °C

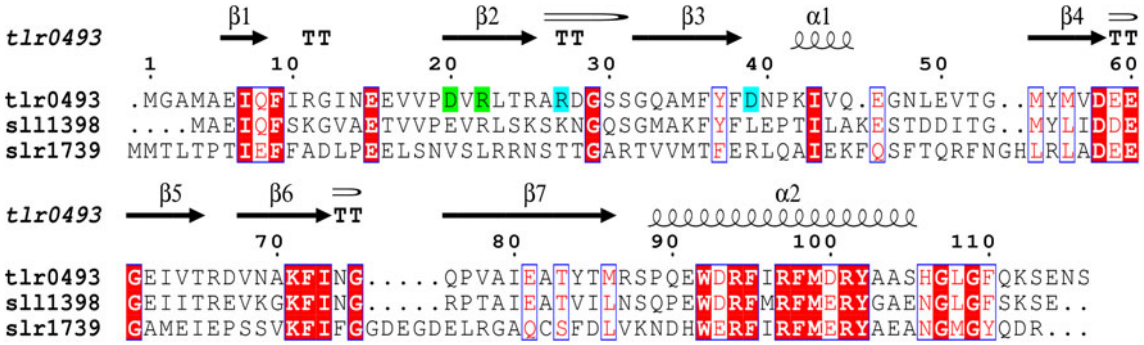

Fig. 1 Sequence alignment of Psb28 from *T. elongatus* (*tlr0493*) and Psb28-1 (*sll1398*) and Psb28-2 (*slr1739*) from *Synechocystis* 6803. Residues involved in salt bridges between different chains in putative dimer are highlighted in green and cyan. The picture was created by ESPript server (Gouet et al. 1999) and β-hairpins (⊃) were detected by ProMotif (Hutchinson and Thornton 1996)

using a Mosquito® robot (TTP LabTech, UK). Rod-shaped Psb28 crystals appeared in sitting drops with the protein solution mixed with an equal volume of 20 % (v/v) PEG200, 20 % (w/v) PEG4000, 10 % (v/v) 2-propanol buffer and 100 mM HEPES sodium salt pH 7.5. A crystal was mounted in a loop and plunged into liquid nitrogen with no further cryoprotection. Data were collected on beamline I04-1 at Diamond Light Source on a Pilatus 6 M detector.

The structure was solved by molecular replacement in PHASER (McCoy et al. 2007). The NMR structure of Psb28-1 from *Synechocystis* (PDB code 2KVO) was truncated to match the *T. elongatus* sequence by CHAINSAW and the first model used as a search model. A partial solution with three copies showed a clear Psb28 dimer. A search with this dimer yielded a clear solution with two dimers in the asymmetric unit. The structure was completed and edited in Coot (Emsley et al. 2010), with cycles of refinement in REFMAC5 (Murshudov et al. 2011) and finally with Phenix (Adams et al. 2010). Non-crystallographic symmetry restraints were applied. The atomic model and structure factors have been deposited in the PDB under accession number 3ZPN.

Growth of *Synechocystis* strains and protein analysis

The glucose-tolerant wild type strain (WT-G) of *Synechocystis* 6803 (Williams 1988) and the previously constructed ΔCP43 (Vermaas et al. 1988), ΔCP43/CP47-His (Boehm et al. 2012b), ΔPSI (Shen et al. 1993), ΔPSI/ΔHliABCD (Vavilin et al. 2007) strains were used in this study. The Hlip- and Psb28-lacking derivatives of the ΔCP43 strain were obtained by the transformation of the ΔCP43 strain using genomic DNA isolated from previously described insertion mutants lacking HliA, HliB (Xu et al., 2002) and Psb28 (Dobakova et al. 2009). Similarly, the PSI-less strain lacking PsbH was obtained by transformation of the ΔPSI strain using genomic DNA isolated from the *psbH* deletion strain (Mayes et al. 1993). The C-terminally flagged strain was constructed by transformation of the WT-G strain by a synthetic construct bearing the nucleotide sequence of *psb28-1* gene fused to a sequence encoding a 3 × *flag* sequence at the C-terminus followed by a zeocine-resistance cassette together with 300-bp upstream and 200-bp downstream region of the original *psb28-1* gene. Strains were grown in liquid BG-11 mineral medium and maintained on solid BG-11 plates containing 1.5 % (w/v) agar, both containing 5 mM *N*-tris (hydroxymethyl)methyl-2-aminoethanesulfonic acid–KOH, pH 8.2, at a light intensity of 40 (for WT-G strains) or 5 (for PSI-less strains) $\mu E\ m^2\ s^{-1}$ of white fluorescent light at 29 °C. The medium was supplemented with 5 mM glucose.

Two-dimensional protein analyses were performed by a combination of blue native and SDS-PAGE as described in Komenda et al. (2012b). 2D gels were stained by Sypro Orange, blotted onto PVDF membranes and probed with specific antibodies against D1, Psb28-1 and Psb28-2 of *Synechocystis* 6803 (Komenda et al. 2012b; Boehm et al. 2012b).

Results and discussion

Sequence alignment

In contrast to *Synechocystis* 6803 which contains two Psb28 homologues, there is only one Psb28 homologue encoded in the *T. elongatus* genome (Fig. S1). Sequence comparisons revealed 59 % identity (78 % similarity) and 33 % identity (57 % similarity) between Psb28 from *T. elongatus* and Psb28-1 and Psb28-2 from *Synechocystis* 6803, respectively (Fig. 1). The full length gene *tlr0493* encoding Psb28 was expressed in *E. coli* as an N-terminal His-tagged derivative (Fig. S2a). After removal of the His-tag by thrombin cleavage (Fig. S2b), to leave two additional Gly-Ser residues at the N-terminus, and concentrating to 32 mg/ml, the protein was crystallised in two crystal forms only one of which

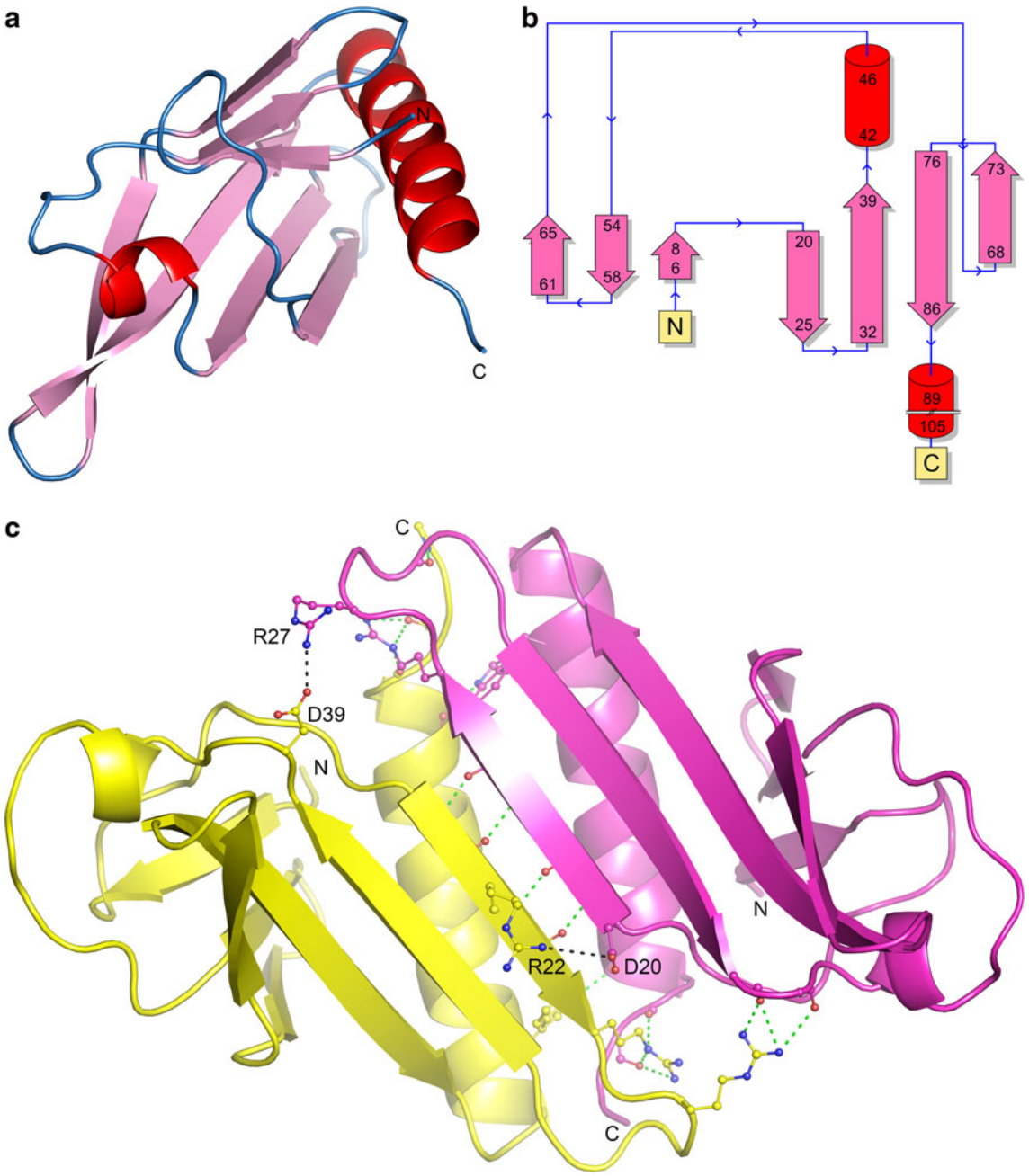

Fig. 2 Structural features of Psb28 from *T. elongatus*. **a** 3D fold of protein **b** its topological cartoon representation and c protein–protein interactions in dimeric Psb28 from *T. elongatus*. Salt bridges and hydrogen bonds are shown as *black* and *green dashed lines*, respectively. For full list of residues involved in H-bonds refer to Table S1

was suitable for structure determination. Size-exclusion chromatography indicated that the *E. coli*-expressed Psb28 used for crystallisation could exist as monomers or dimers depending on the buffer (Fig. S2c and d).

Structure description

The best X-ray diffraction data sets were collected for crystals obtained in 20 % (v/v) PEG200, 20 % (w/v) PEG4000, 10 % (v/v) 2-propanol buffer and 100 mM HEPES sodium salt pH 7.5 (Fig. S3a) and the structure was solved by molecular replacement using the NMR structure of Psb28-1 from *Synechocystis* 6803 (PDB: 2KVO); Table 1 shows the data collection and refinement statistics. The structure reveals that β-strands and α-helices account for 44 and 20 % of Psb28, respectively (Fig. 2). Two antiparallel β-sheets (A and B) are composed of β-strands, β1-4-5 and β2-3-6-7, with β-hairpins connecting β2 and β3, β4 and β5 and β6 and β7. One inverse

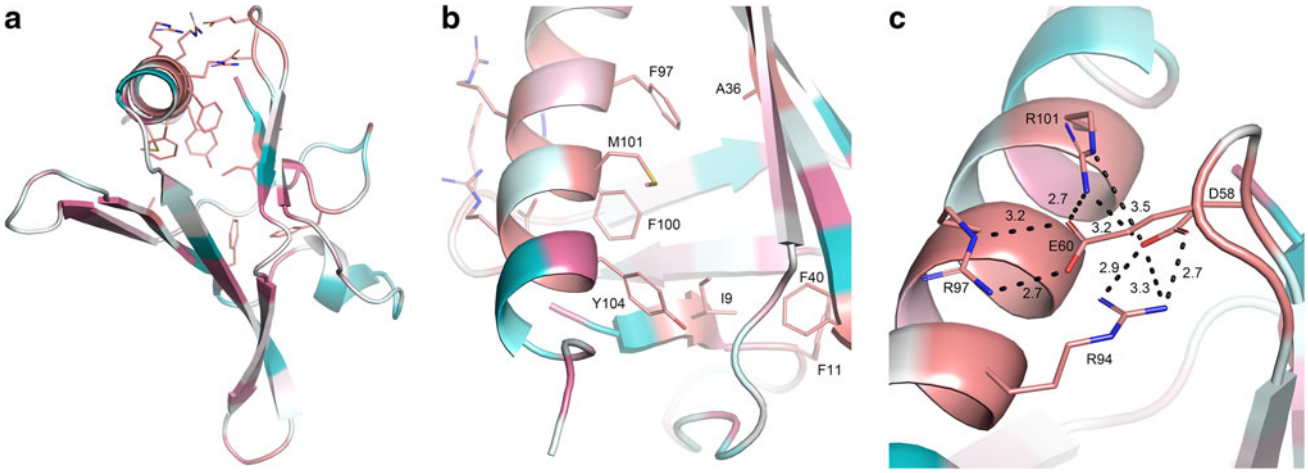

Fig. 3 Analysis of conserved residues distribution between cyanobacterial, algal and plant Psb28-1 and cyanobacterial Psb28-2 as calculated by Consurf (Ashkenazy et al. 2010). **a** Side chains of the most conserved residues are shown as sticks. **b** Side chains (shown as *sticks*) of conserved residues lining the hydrophobic core of the protein. **c** Interactions between the two absolutely conserved regions found in both the Psb28-1 and Psb28-2 with lengths given in Å. The conservation colouring scale spans from teal for variable to salmon for the most conserved residues. Compare with sequence alignment from Fig. 1

γ-turn is present ($Arg_{66}Asp_{67}Val_{68}$) between β5 and β6 (Fig. 1). Two α-helices are present, one short consisting of five residues (Lys_{42}-Glu_{46}) and one longer of 17 residues (Pro_{89}-Ser_{105}). The former is located between β3 and β4 and the latter is close to the C-terminus. The first 2 and last 6 residues are missing from electron density so that only residues 3–110 were modelled.

Comparison with the solution structure of *Synechocystis* Psb28-1

Structural comparison between the Psb28 crystal structure presented here, and Psb28-1 revealed a high overall similarity with a pairwise C_α RMSD of 1.6 Å as calculated by SSM (Krissinel and Henrick 2004). As shown in Fig. S4, the most significant difference between both the proteins lies in the loop between β-strands 3 and 4 (see below). In addition, Psb28 from *T. elongatus* lacks a 3_{10} helix composed of residues 39–41 (2KVO original numbering) and the second 3_{10} helix of Psb28-1 is replaced by a five-residue long α-helix (Lys_{42}-Glu_{46}). Only one significant hit, Psb28-1, with a Z score of 13.8, was detected by DALI analysis (Holm and Rosenstrom 2010).

In the crystal structure, four molecules are present in the asymmetric unit (Fig. S3b). As suggested by PISA (Krissinel and Henrick 2007), and in contrast to the solution structure of His-tagged Psb28-1 from *Synechocystis* 6803, Psb28 from *T. elongatus* forms two dimers composed of chains A–B and C–D. The interface is created between long C-terminal α-helices and β-strands 2 with numerous hydrogen bonds between chains (Table S1). Two salt bridges (Asp_{20}-Arg_{22} and Arg_{27}-Asp_{39}) further stabilize the dimer (Fig. 2c).

Table 1 Data collection and refinement statistics for the Psb28 crystal structure

Crystal parameters	
Space group	$P\ 4_3$
Cell dimensions	$a = b = 57.06$ Å $c = 183.32$ Å $\alpha = \beta = \gamma = 90^\circ$
Data collection	
Beamline	Diamond Light Source I04–1
Wavelength (Å)	0.92000
Resolution (Å)	2.36–57.06 (2.42–2.36)
Unique observations	23633 (1702)
R_{merge}	0.05 (0.55)
Mean ($< I > / \sigma I$)	13.2 (1.75)
Completeness (%)	98.7 (97.6)
Multiplicity	3.1 (2.9)
Refinement	
R_{work}/R_{free} (%)	19.45/23.42
Number of protein residues	427
RMSD stereochemistry	
Bond lengths (Å)	0.009
Bond angles (°)	1.339
Ramachandran analysis (%)	
Residues in outlier regions	0.48
Residues in favoured regions	98.3
Residues in allowed regions	99.5

Numbers in parentheses refer to the outermost resolution shell

$R_{merge} = \Sigma\ |I - < I > | / \Sigma\ I$ where I is the integrated intensity of a given reflection and $< I >$ is the mean intensity of multiple corresponding symmetry-related reflections

$R_{work} = \Sigma\ ||F_o| - |F_c|| / \Sigma\ F_o$ where F_o and F_c are the observed and calculated structure factors respectively

$R_{free} = R_{work}$ calculated using ~5 % random data excluded from the refinement

RMSD stereochemistry is the deviation from ideal values

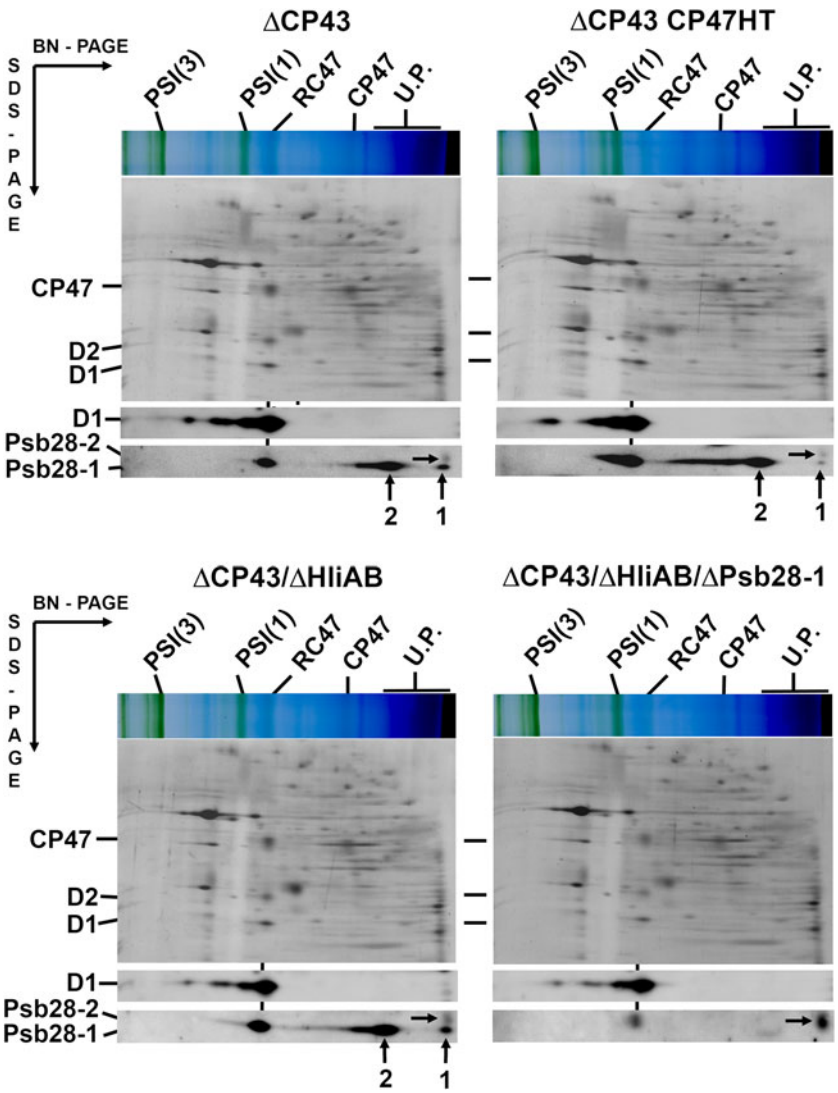

Fig. 4 The occurrence of the monomeric and dimeric forms of Psb28-1 protein in various CP43-less strains. Membranes isolated from the strains cultivated under 10 μmol photons m^{-2} s^{-1} in the presence of 5 mM glucose were analysed by 2D CN/SDS-PAGE. The gel was stained by Sypro Orange and then blotted to PVDF membrane which was probed by antibodies specific to D1, D2 and Psb28-1. The dimeric (2) and monomeric (1) forms of Psb28 are designated by *vertical arrows*. For comparison, signals of Psb28-2 protein corresponding to the monomer obtained using a specific antibody are also shown and designated by *horizontal arrows*. The loaded samples contained 5 μg of Chl

Sequence alignments suggest that a salt bridge may also be present between Glu_{17} and Arg_{19} of Psb28-1 from *Synechocystis* 6803. Our structural analysis also suggests that a second salt bridge might form between Lys_{24} and Glu_{37} of Psb28-1 despite the fact that the loop with Lys_{24} adopts different conformations to the corresponding region in the protein from the thermophilic cyanobacterium. In fact, the flexibility of this region may result from the lack of the stabilizing effect of an intradimeric salt bridge. Based on a structural alignment of the C-terminally tagged Psb28-1 monomer and the Psb28 dimer described here, we speculate that the presence of the His-tag at the C-terminus of Psb28 might impede dimerization (Fig. S5).

Analysis of conserved residues and implications for the structure of Psb28-2

Using the crystal structure of Psb28 from *T. elongatus* described here and sequences of cyanobacterial, algal and plant Psb28-1 and cyanobacterial Psb28-2, we mapped conserved residues on the protein structure using a Consurf analysis (Fig. 3a). This analysis revealed that the conserved hydrophobic residues shown in Fig. 3b create a hydrophobic core inside Psb28 and that most conserved residues are located in two clusters of charged residues. One of them, a patch of acidic residues, forms a β-turn between β4 and β5, whereas the other, composed of basic residues, is found in the middle part of the long C-terminal α-helix. Interestingly, these two clusters interact with each other by means of intramolecular hydrogen bonds and salt bridges (Fig. 3c). By bridging two distant parts of the protein. these interactions seem to enable the formation of the hydrophobic core and probably stabilize the protein structure. Given the relatively high sequence similarity between Psb28-1 and Psb28-2 and that sequences of both the protein sub-families were taken into consideration, this analysis supports the idea that Psb28-2 adopts a very similar 3D fold to Psb28-1.

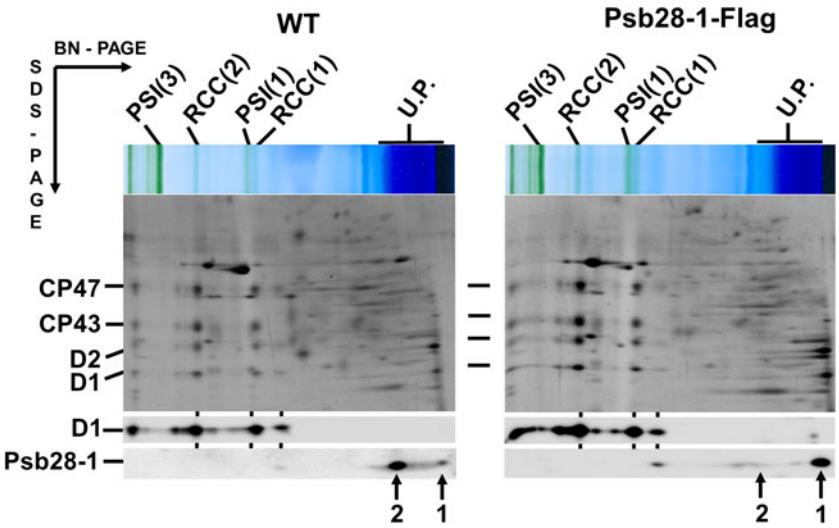

Fig. 5 The occurrence of the monomeric form of Psb28-1 in the strain expressing the C-terminally Flagged Psb28-1 protein. Membranes isolated from both the strains were analysed by 2D BN/SDS-PAGE. The gel was stained by Sypro Orange and then blotted to PVDF membrane which was probed by antibodies specific to D1 and Psb28-1. The dimeric (*2*) and monomeric (*1*) forms of Psb28-1 are designated by *vertical arrows*. The loaded samples contained 5 μg of Chl

Analysis of Psb28-1 and Psb28-2 in *Synechocystis* 6803

To explore the possibility that Psb28-1 and Psb28-2 of *Synechocystis* 6803 might exist in different oligomeric states in vivo, we separated detergent-solubilised membrane protein extracts by BN-PAGE in the first dimension and by SDS-PAGE in the second dimension, followed by immunoblotting using antibodies specific for Psb28-1 and Psb28-2 (Fig. 4). Using this technique, three distinct populations of Psb28-1 were detected. As reported previously some of the Psb28-1 co-migrated with the RC47 complex that accumulates in ΔCP43 mutants (Dobakova et al. 2009; Boehm et al. 2012b), but most (band 2 in Fig. 4) migrated with an apparent molecular mass distinctly larger than that of 'unassembled' Psb28-2 present in all strains but most abundant in the ΔPsb28-1 strain (Fig. 4). Some Psb28-1 did co-migrate with Psb28-2 (band 1 in Fig. 4), but its abundance was variable between samples and sometimes not detected (Boehm et al. 2012b). Control immunoblots confirmed that band 2 of Psb28-1 did not co-migrate with the CP47 subunit (data not shown), and its migration was unaffected in strains lacking either PsbH or four members of the Hli protein family (HliA-D), two of which are known to attach to RC47 under high-light conditions (Fig. S6) (Yao et al. 2007). Together these data suggest that band 2 is probably an oligomer. According to the crystal structure (Fig. S5), dimerisation of Psb28-1 is potentially impaired by addition of a tag at the C-terminus of Psb28-1. Consistent with this hypothesis, a C-terminal 3xFlag-tag derivative of Psb28-1 expressed in *Synechocystis* 6803 now migrated mainly as a monomer (band 1) in the same region of the BN gel as Psb28-2 (Fig. 5).

Conclusion

In summary, we have determined the crystal structure of Psb28 from *T. elongatus* and have provided evidence that Psb28-1, but not Psb28-2, of *Synechocystis* 6803 forms a higher order structure, most likely a dimer, in vivo. The physiological importance of Psb28-1 dimerisation is currently unknown. Our data provide a structural model for how Psb28-1 might oligomerise in vivo which can be tested in the future by mutagenesis. The crystal structure determined here might prove to be useful in determining the site of attachment of Psb28 to PSII determined through cross-linking experiments.

Acknowledgments The authors would like to thank the Biotechnology and Biological Sciences Research Council (BBSRC) for financial support (Grant BB/I00937X/1). JWM holds a BBSRC David Phillips Fellowship (BB/F023308/1). JK and MB were supported by projects Algatech (CZ.1.05/2.1.00/03.0110), RVO61388971 and P501/11/0377 of the Grant Agency of the Czech Republic. The authors wish to thank the staff of the Diamond Light Source for their assistance.

References

Adams PD, Afonine PV, Bunkoczi G, Chen VB, Davis IW, Echols N, Headd JJ, Hung LW, Kapral GJ, Grosse-Kunstleve RW, McCoy AJ, Moriarty NW, Oeffner R, Read RJ, Richardson DC, Richardson JS, Terwilliger TC, Zwart PH (2010) PHENIX: a comprehensive Python-based system for macromolecular structure solution. Acta Crystallogr D 66:213–221

Adir N, Zer H, Shochat S, Ohad I (2003) Photoinhibition—a historical perspective. Photosynth Res 76:343–370

Ashkenazy H, Erez E, Martz E, Pupko T, Ben-Tal N (2010) ConSurf 2010: calculating evolutionary conservation in sequence and structure of proteins and nucleic acids. Nucleic Acids Res 38:W529–W533

Boehm M, Romero E, Reisinger V, Yu J, Komenda J, Eichacker LA, Dekker JP, Nixon PJ (2011) Investigating the early stages of photosystem II assembly in *Synechocystis* sp. PCC 6803: isolation of CP47 and CP43 complexes. J Biol Chem 286:14812–14819

Boehm M, Yu J, Krynicka V, Barker M, Tichy M, Komenda J, Nixon PJ, Nield J (2012a) Subunit organization of a *Synechocystis* hetero-oligomeric thylakoid FtsH complex involved in photosystem II repair. Plant Cell 24:3669–3683

Boehm M, Yu J, Reisinger V, Beckova M, Eichacker LA, Schlodder E, Komenda J, Nixon PJ (2012b) Subunit composition of CP43-less photosystem II complexes of *Synechocystis* sp. PCC 6803: implications for the assembly and repair of photosystem II. Philos Trans R Soc Lond B Biol 367:3444–3454

Chi W, Ma J, Zhang L (2012) Regulatory factors for the assembly of thylakoid membrane protein complexes. Philos Trans R Soc Lond B Biol 367:3420–3429

Dobakova M, Tichy M, Komenda J (2007) Role of the PsbI protein in photosystem II assembly and repair in the cyanobacterium *Synechocystis* sp. PCC 6803. Plant Physiol 145:1681–1691

Dobakova M, Sobotka R, Tichy M, Komenda J (2009) Psb28 protein is involved in the biogenesis of the photosystem II inner antenna CP47 (PsbB) in the cyanobacterium *Synechocystis* sp. PCC 6803. Plant Physiol 149:1076–1086

Emsley P, Lohkamp B, Scott WG, Cowtan K (2010) Features and development of Coot. Acta Crystallogr D 66:486–501

Ferreira KN, Iverson TM, Maghlaoui K, Barber J, Iwata S (2004) Architecture of the photosynthetic oxygen-evolving center. Science 303:1831–1838

Gouet P, Courcelle E, Stuart DI, Metoz F (1999) ESPript: analysis of multiple sequence alignments in postscript. Bioinformatics 15:305–308

Guskov A, Kern J, Gabdulkhakov A, Broser M, Zouni A, Saenger W (2009) Cyanobacterial photosystem II at 2.9-Å resolution and the role of quinones, lipids, channels and chloride. Nat Struct Mol Biol 16:334–342

Holm L, Rosenstrom P (2010) Dali server: conservation mapping in 3D. Nucl Acids Res 38:W545–W549

Hutchinson EG, Thornton JM (1996) PROMOTIF–a program to identify and analyze structural motifs in proteins. Protein Sci 5:212–220

Kamiya N, Shen JR (2003) Crystal structure of oxygen-evolving photosystem II from *Thermosynechococcus vulcanus* at 3.7-Å resolution. Proc Natl Acad Sci USA 100:98–103

Komenda J, Reisinger V, Muller BC, Dobakova M, Granvogl B, Eichacker LA (2004) Accumulation of the D2 protein is a key regulatory step for assembly of the photosystem II reaction center complex in *Synechocystis* PCC 6803. J Biol Chem 279:48620–48629

Komenda J, Kuvikova S, Granvogl B, Eichacker LA, Diner BA, Nixon PJ (2007) Cleavage after residue Ala352 in the C-terminal extension is an early step in the maturation of the D1 subunit of Photosystem II in *Synechocystis* PCC 6803. Biochim Biophys Acta 1767:829–837

Komenda J, Sobotka R, Nixon PJ (2012a) Assembling and maintaining the Photosystem II complex in chloroplasts and cyanobacteria. Curr Opin Plant Biol 15:245–251

Komenda J, Knoppova J, Kopecna J, Sobotka R, Halada P, Yu J, Nickelsen J, Boehm M, Nixon PJ (2012b) The Psb27 assembly factor binds to the CP43 complex of photosystem II in the cyanobacterium *Synechocystis* sp. PCC 6803. Plant Physiol 158:476–486

Krissinel E, Henrick K (2004) Secondary-structure matching (SSM), a new tool for fast protein structure alignment in three dimensions. Acta Crystallogr D 60:2256–2268

Krissinel E, Henrick K (2007) Inference of macromolecular assemblies from crystalline state. J Mol Biol 372:774–797

Liu H, Roose JL, Cameron JC, Pakrasi HB (2011) A genetically tagged Psb27 protein allows purification of two consecutive photosystem II (PSII) assembly intermediates in *Synechocystis* 6803, a cyanobacterium. J Biol Chem 286:24865–24871

Loll B, Kern J, Saenger W, Zouni A, Biesiadka J (2005) Towards complete cofactor arrangement in the 3.0 Å resolution structure of photosystem II. Nature 438:1040–1044

Mayes SR, Dubbs JM, Vass I, Hideg E, Nagy L, Barber J (1993) Further characterization of the *psbH* locus of *Synechocystis* sp. PCC 6803: inactivation of *psbH* impairs Q_A to Q_B electron transport in photosystem 2. Biochemistry 32:1454–1465

McCoy AJ, Grosse-Kunstleve RW, Adams PD, Winn MD, Storoni LC, Read RJ (2007) Phaser crystallographic software. J Appl Crystalogr 40:658–674

Michoux F, Takasaka K, Boehm M, Nixon PJ, Murray JW (2010) Structure of CyanoP at 2.8 Å: implications for the evolution and function of the PsbP subunit of photosystem II. Biochemistry 49:7411–7413

Michoux F, Takasaka K, Boehm M, Komenda J, Nixon PJ, Murray JW (2012) Crystal structure of the Psb27 assembly factor at 1.6 Å: implications for binding to Photosystem II. Photosynth Res 110:169–175

Murshudov GN, Skubak P, Lebedev AA, Pannu NS, Steiner RA, Nicholls RA, Winn MD, Long F, Vagin AA (2011) REFMAC5 for the refinement of macromolecular crystal structures. Acta Crystallogr D 67:355–367

Nixon PJ, Trost JT, Diner BA (1992) Role of the carboxy terminus of polypeptide D1 in the assembly of a functional water-oxidizing manganese cluster in photosystem II of the cyanobacterium *Synechocystis* sp. PCC 6803: assembly requires a free carboxyl group at C-terminal position 344. Biochemistry 31:10859–10871

Nixon PJ, Michoux F, Yu J, Boehm M, Komenda J (2010) Recent advances in understanding the assembly and repair of photosystem II. Ann Bot 106:1–16

Nowaczyk MM, Krause K, Mieseler M, Sczibilanski A, Ikeuchi M, Rogner M (2012) Deletion of *psbJ* leads to accumulation of Psb27-Psb28 photosystem II complexes in *Thermosynechococcus elongatus*. Biochim Biophys Acta 1817:1339–1345

Promnares K, Komenda J, Bumba L, Nebesarova J, Vacha F, Tichy M (2006) Cyanobacterial small chlorophyll-binding protein ScpD (HliB) is located on the periphery of photosystem II in the vicinity of PsbH and CP47 subunits. J Biol Chem 281:32705–32713

Sakata S, Mizusawa N, Kubota-Kawai H, Sakurai I, Wada H (2013) Psb28 is involved in recovery of photosystem II at high temperature in *Synechocystis* sp. PCC 6803. Biochim Biophys Acta 1827:50–59

Shen G, Boussiba S, Vermaas WFJ (1993) *Synechocystis* sp. PCC 6803 strains lacking photosystem I and phycobilisome function. Plant Cell 5:1856–1863

Umena Y, Kawakami K, Shen JR, Kamiya N (2011) Crystal structure of oxygen-evolving photosystem II at a resolution of 1.9 Å. Nature 473:55–60

Vavilin D, Yao D, Vermaas W (2007) Small Cab-like proteins retard degradation of photosystem II-associated chlorophyll in *Synechocystis* sp. PCC 6803: kinetic analysis of pigment labeling with ^{15}N and ^{13}C. J Biol Chem 282:37660–37668

Vermaas WFJ, Ikeuchi M, Inoue Y (1988) Protein composition of the photosystem II core complex in genetically engineered mutants of the cyanobacterium *Synechocystis* sp. PCC 6803. Photosynth Res 17:97–113

Williams JGK (1988) Construction of specific mutations in PSII photosynthetic reaction center by genetic engineering methods in *Synechocystis* 6803. Methods Enzymol 167:766–778

Xu H, Vavilin D, Funk C, Vermaas W (2002) Small Cab-like proteins regulating tetrapyrrole biosynthesis in the cyanobacterium *Synechocystis* sp. PCC 6803. Plant Mol Biol 49:149–160

Yang Y, Ramelot TA, Cort JR, Wang D, Ciccosanti C, Hamilton K, Nair R, Rost B, Acton TB, Xiao R, Everett JK, Montelione GT, Kennedy MA (2011) Solution NMR structure of photosystem II reaction center protein Psb28 from *Synechocystis* sp. Strain PCC 6803. Proteins 79:340–344

Yao D, Kieselbach T, Komenda J, Promnares K, Prieto MA, Tichy M, Vermaas W, Funk C (2007) Localization of the small CAB-like proteins in photosystem II. J Biol Chem 282:267–276